PAPER

Check for updates

Fabrication of fine-pored polydimethylsiloxane using an isopropyl alcohol and water mixture for adjustable mechanical, optical, and thermal properties†

Yeunjun Kwak,‡ Yunsung Kang,‡ Wonkeun Park, Eunhwan Jo and Jongbaeg Kim ID *

Porous polydimethylsiloxane (PDMS) has garnered interest owing to its large inner surface area, high deformability, and lightweight, while possessing inherent properties, such as transparency, flexibility, cost-effectiveness, ease of fabrication, chemical/mechanical stability, and biocompatibility. For producing porous PDMS, gas foaming, sacrificial template, and emulsion template techniques have been used extensively. However, the aforementioned methods have difficulty in achieving submicron-sized inner pores, which is advantageous for improving flexibility and transparency. This study demonstrates a simple fabrication method for obtaining porous PDMS with fine pores partially down to the sub-micron scale. This is possible by the use of cheap, volatile, and easily accessible isopropyl alcohol (IPA) as a co-solvent in water and pre-PDMS emulsion. IPA shows an affinity towards both water and prepolymer, resulting in an increased distribution of small water particles inside PDMS before curing. These water particles evaporate while curing the prepolymer emulsion, thereby generating fine pores. The fine size and number density of pores are controlled by water and the added amount of IPA, resulting in adjustable mechanical, optical, and thermal properties of porous PDMS.

Introduction

Numerous flexible and transparent electronics have evolved for promising technologies including smart displays, electronic skin, human–machine interfaces, and wearable devices. In recent decades, numerous studies primarily focused on developing electrical conductors,[1,2] thin-film transistors,[3,4] light-emitting diodes,[5,6] chemical sensors,[7,8] and strain/pressure sensors[9–11] for the above-mentioned high-end applications requiring flexibility and transparency. However, this was not possible without the introduction of flexible and transparent polymer substrates, which enabled electronic devices to overcome the limitations of rigid and opaque electronics based on silicon processing. Polydimethylsiloxane (PDMS), polyethylene terephthalate, and polyimide have been frequently used as substrate materials. Among them, PDMS has attracted much interest owing to its transparency, flexibility, cost-effectiveness, ease of fabrication, chemical/mechanical stability, and biocompatibility.[12–14]

One of the strategies using PDMS with the abovementioned characteristics is endowing its porosity inside. This makes it

School of Mechanical Engineering, Yonsei University, 50 Yonsei-ro, Seodaemun-gu, Seoul, 03722, Republic of Korea. E-mail: kimjb@yonsei.ac.kr

† Electronic supplementary information (ESI) available. See DOI: 10.1039/d1ra02466c

‡ Y. Kwak and Y. Kang equally contributed this work.

possible for PDMS to have additional properties, such as large surface area, high deformability, and lightweight, to originate from the inner porous structure. There are five representative methods for producing porous structures in PDMS, *i.e.*, sacrificial template-, gas foaming-, 3D printing-, phase separation-, and emulsion template-based techniques.[15] Although the particle leaching method that uses sugar or salt particles as the sacrificial template is the most popular,[16–23] emulsion template techniques mixing water with uncured prepolymer have also been explored significantly.[24–32] Water molecules are aggregated and distributed separately inside the PDMS prepolymer, *i.e.*, it behave as oil during a curing process. Additionally, water vapor can easily evaporate and permeate through PDMS at the curing temperature,[33] resulting in the formation of an inner porous structure, *i.e.*, water acts as a porogen when fabricating porous PDMS. This method allows the formation of either interconnected or isolated pore structures. Open-cell porous PDMS with a continuous inner channel has gained significant interest owing to their various applications, including flexible conductors,[34] oil absorbents,[27,35] microfluidics,[36] cell culture,[18,37] capacitive pressure sensor,[38] and triboelectric energy harvester.[39] However, there is a lack of applications utilizing closed-cell porous PDMS. Additionally, to the best of our knowledge, an approach using porous PDMS for its characterization as a flexible and transparent substrate has not yet been reported.

In this study, we demonstrate a method for producing fine-pored PDMS. In this method, isopropyl alcohol (IPA) was used

as an additional solvent and introduced into the emulsion with pre-PDMS and DI water, thereby resulting in the reduced size and increased number density of pores. This enables the formation of submicron-sized pores, which was rarely achieved *via* emulsion template techniques.[15] Furthermore, we propose and explain a pore-generation mechanism in the emulsion template method when IPA is added to water and PDMS. The number and size of pores obtained for different weight ratios of IPA to PDMS were analysed using an image-processing technique, and the effect of various solvents in conjunction with deionized water on the formation of porous PDMS was also evaluated. Finally, we demonstrated that the mechanical flexibility, optical transparency, and thermal diffusivity of porous PDMS can be adjusted by varying the added weight ratio of IPA to water and prepolymer emulsion. Additionally, the reduced pore size and increased number density allows closed-cell porous PDMS to exhibit improved flexibility and transparency, which could be advantageous when utilized as a flexible and transparent substrate.

Experimental methods

Fabrication of porous PDMS

Fig. 1 shows the fabrication process of porous PDMS in this study.[40] First, a PDMS base (Sylgard 184A, Dow Corning) was mixed with a curing agent (Sylgard 184B, Dow Corning) at a weight ratio of 10 : 1. DI water and IPA were poured simultaneously into the uncured PDMS at weight ratios of 5 : 100 and 0/1 : 100/5 : 100/10 : 100, respectively. Subsequently, the PDMS/DI water/IPA emulsion was vigorously blended for 1 min at 500 rpm using a mechanical stirrer. The emulsion was placed in a customized vacuum chamber for 30 min to remove the air bubbles generated unintentionally inside itself. Next, the emulsion was placed in a Petri dish and cured in a convection oven at 70 °C for 1 h. The cured PDMS

was placed in an ambient environment for one day at room temperature to completely remove any solvents that may remain inside. Finally, PDMS was carefully prepared into various dimensions for a particular purpose.

Characterization of porous PDMS

To investigate the distribution of pores in PDMS, a cross-section of the specimen was subjected to scanning electron microscopy (SEM, IT-500HR, JEOL). The diameter and number of pores were evaluated from cross-sectional SEM images using a software program (Image J).[41] The pore size was determined using Feret's diameter, which is the longest distance between two arbitrary points along each pore.[42] The mechanical properties of porous PDMS were investigated using a universal testing machine (UTM, OTT-001, ORIENTALTM) equipped with both a displacement sensor and a load cell with a capacity of 100 N. The prepared porous PDMS had a volume of $1 \times 1 \times 1.25$ cm^3 for the compressive tests conducted at a speed of 2 mm min^{-1}. The optical transmittance and haze of various specimens having a thickness of 3 mm were examined in the visible light spectrum using a UV/vis spectrometer (V-650, JASCO Cooperation) and a spectrophotometer (CM-3600d, Konica Minolta), respectively. Thermal diffusivity of the 1.25 mm thick porous PDMS was measured by the laser flash method using a commercial equipment (LFA-457, NETZSCH) at elevated temperatures ranging from 40 to 120 °C.

Results and discussion

Fine pore formation using IPA and water mixture into PDMS

PDMS is well known as a hydrophobic material and it is not easily miscible with water without a vigorous mixing procedure to form an emulsion. However, this hydrophobicity also contributes to the formation of porogens of various sizes ranging from tens to several microns depending on the weight ratio of mixed water when fabricating porous PDMS.[29] However,
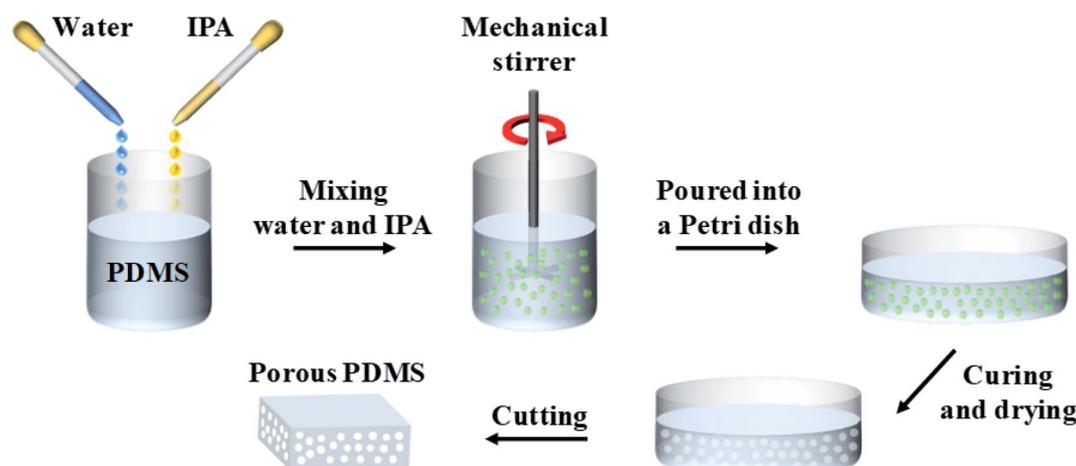
Fig. 1 Fabrication process of porous PDMS. PDMS base was mixed with the curing agent at a weight ratio of 10 : 1. Subsequently, DI water and IPA were simultaneously poured into the uncured PDMS at the weight ratio of 5 : 100 and 10 : 100, respectively. The PDMS/DI water/IPA emulsion was blended vigorously for 1 min at 500 rpm using a mechanical stirrer. The emulsion was placed in a customized vacuum chamber for 30 min to remove air bubbles that were generated unintentionally inside the sample. Then, the emulsion was poured into a Petri dish and cured in a convection oven at 70 °C for 1 h. The cured PDMS was placed in an ambient environment for one day at room temperature to completely remove any solvents may remain inside.
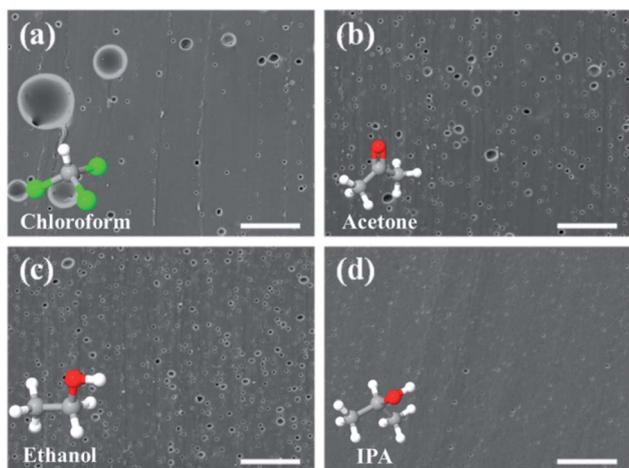
Fig. 2 Cross-sectional SEM images of porous PDMS prepared using water and (a) chloroform, (b) acetone, (c) ethanol, and (d) isopropanol (scale bar: 50 μm).

the pore sizes with this range reduces the transparency of porous PDMS significantly due to light scattering.[26]

This makes it difficult for porous PDMS to be used for applications requiring transparency. To overcome this issue, it is necessary to develop porous PDMS with enhanced transparency by reducing the pore size down to the submicron level. Hence, we used a cheap, volatile, and easily accessible solvent,

whose properties showed an affinity towards water and PDMS. This would result in the formation of minute water particles inside PDMS upon emulsification. To confirm our approach, various solvents were added to the pre-PDMS and water mixture, including chloroform, acetone, ethanol, and IPA. The added weight ratio of water and IPA to PDMS was fixed at 5 : 100 and 10 : 100, respectively. The added weight of other solvents was adjusted to the same number of moles as that of IPA to PDMS. The SEM images of various fabricated porous PDMS are shown in Fig. 2. Table 1 shows various properties of the selected solvents as a co-solvent.[43–46] Chloroform is hardly soluble in water, which makes it ineffective in reducing the pore size. On the other hand, the use of acetone, ethanol, and IPA as co-solvents were efficient in reducing the pore size in PDMS when compared with the results obtained using water alone (Fig. 3a). This is because of the lowered surface tension of a completely miscible mixture of water and solvent.[47] Among these mixtures, IPA showed the best result to achieve the smallest pore size in PDMS. This could be due to the relatively high swelling ratio of IPA to PDMS and moderate polarity to water. A higher swelling ratio of IPA could indicate that a solvent is more likely to spread inside PDMS. Additionally, the relatively lower polarity of IPA compared to that of ethanol and acetone could induce more possibilities for IPA molecules to be located between polar water and nonpolar pre-PDMS. This makes it easy to spread water particles. The solubility, surface

Table 1 Various properties of selected solvents

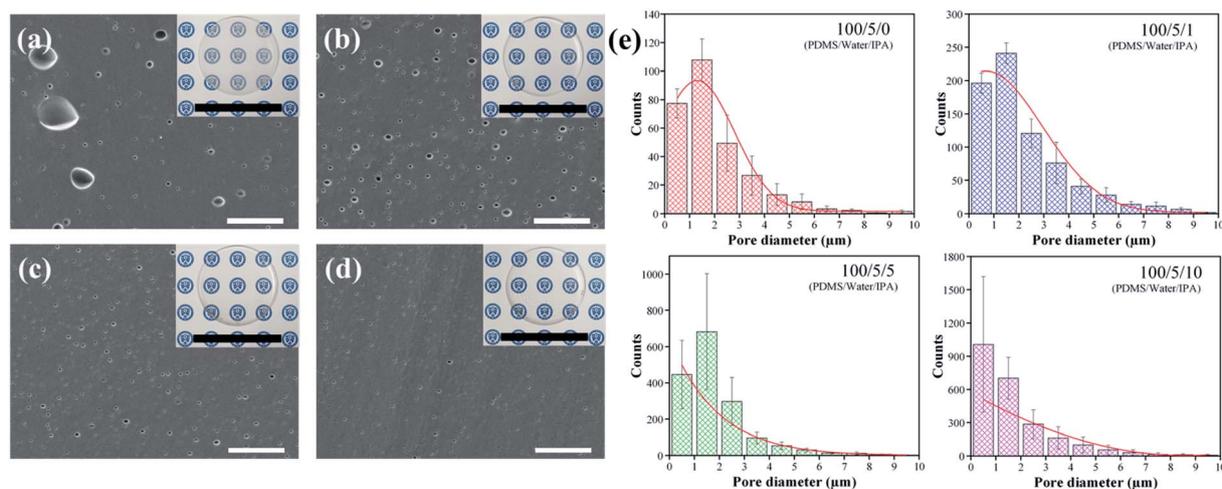| Solvent	Solubility in water	Surface tension (mN m^{-1})	Swelling ratio to PDMS	Relative polarity to water
Chloroform	0.8 g/100 g	26.7	1.39	0.259
Ethanol	Completely miscible	22.0	1.04	0.654
Acetone	Completely miscible	23.0	1.06	0.655
Isopropanol	Completely miscible	23.3	1.09	0.546
Water	—	72.8	1.00	1

Fig. 3 Cross-sectional SEM images of porous PDMS prepared using the added weight ratio of water to PDMS (5 : 100) with (a) 0, (b) 1 : 100, (c) 5 : 100, and (d) 10 : 100 IPA to PDMS (scale bar: 50 μm). Photographs of each sample are shown in the inset (scale bar: 10 cm). (e) Pore size distribution of porous PDMS from an image processing technique. Red lines indicate Gaussian distribution of the pore size.

tension, swelling ratio, and polarity of the solvent as a co-solvent should be considered together to adjust the pore size in porous PDMS. However, porous PDMS was not developed when only a solvent was used without water, as shown in Fig. S1.† This indicates the crucial role of water in the emulsion template technique for fabricating porous PDMS. Fig. 3a–d show the cross-sectional SEM images of porous PDMS prepared using emulsions with the weight ratio of water (5 : 100) and IPA (0, 1 : 100, 5 : 100, and 10 : 100) to PDMS, respectively. The inset images of Fig. 3a–d display the optical images of fabricated PDMS. It was confirmed that the addition of IPA is highly effective for reducing the inner pore size, thereby resulting in an increase in transparency of PDMS, as shown in the inset images. The SEM images of porous PDMS at a low magnification are also presented in Fig. S2.†

The average pore sizes were calculated to be 2.12, 2.07, 1.68, and 1.37 μm in Fig. 3a–d when the added weight ratio of IPA to PDMS was 0, 1 : 100, 5 : 100, and 10 : 100, respectively. The number of pores counted from the four different samples using an image processing technique is presented as a histogram and Gaussian distribution in Fig. 3e. In addition, Fig. S3† presents the distribution of pore size in the relatively small range, and Table S1† shows the average size and its standard deviation of pores in the samples of Fig. 3e. The size and the number of pores decreases and increases quantitatively, respectively, and this tendency corresponds with the observed SEM images. Notably, we achieved a part of submicron-sized fine pores by adding an easily accessible and volatile co-solvent to the emulsion unlike most of the reported studies based on the emulsion template technique showing the pore size down to several microns.[15] Additionally, the usage of IPA as a co-solvent is highly beneficial in that it does not persist inside and does not affect the property of porous PDMS after polymerization when considering that volatile organic compounds show high permeability to PDMS.[48,49] Fig. S4† shows an enlarged cross-sectional SEM image of porous PDMS prepared with the added weight ratio of water (5 : 100) and IPA (10 : 100) to PDMS. The manually measured pore size was also distributed around 1 μm, which is consistent with the image processing analysis. Furthermore, a self-stratifying porous structure with a non-

porous skin layer[32] was also observed in our sample, as shown in Fig. S5,† originating from the relatively rapid evaporation of water at the surface. This structure is worth mentioning that various patterning strategies can be integrated on the top surface of the fabricated porous PDMS retaining transparency and flexibility. Another considerable aspect, when this skin layer is formed, is the effect of gravity to water droplet. When considering the effect of gravity on the water droplet in PDMS emulsion, Stoke's law can be applied.[32,50] According to Stoke's law, the speed of water droplet sedimentation is expressed as an eqn (1) where V_{stokes}, ρ_w, ρ_p, g, d, and μ_p represent the sedimentation velocity, water density (1 g cm^{-3}), liquid PDMS density (0.98 g cm^{-3}), the acceleration due to the gravity (9.8 m s^{-2}), the particle diameter, and the dynamic viscosity of PDMS (3.5 Pa s, Sylgard 184), respectively.

$$V_{stokes} = \frac{(\rho_w - \rho_p)gd^2}{18\mu_p} \quad (1)$$

For example, when the diameter of water particle is 10 μm, the descent velocity of it is calculated as approximately 0.3 nm s^{-1}. The calculated displacement of water particle is approximately 1.1 μm for the curing time (1 h). Thus, the effect of gravity on water particles would be negligible to the formation of skin layer.

Mechanical, optical, and thermal properties of porous PDMS

Compressive stress–strain curves of porous PDMS with respect to the weight ratio of added IPA are presented in Fig. 4. The hysteresis phenomena of porous PDMS between loading and unloading stresses originate from the viscoelastic behavior of polymers.[51] As the size and number of pores decreased and increased, respectively, we observed a tendency of increased flexibility in closed-cell porous PDMS. Generally, open-cell porous polymers are more flexible than closed-cell polymers because entrapped air can easily escape from interconnected pores when compressed.[52] Likewise, the free volume of pores in closed-cell porous PDMS decreases due to its air permeability when the physical pressure is applied.[53] Thus, the reduced size and the increased number of pores could make it easy for entrapped air to escape from PDMS, resulting in the enhanced
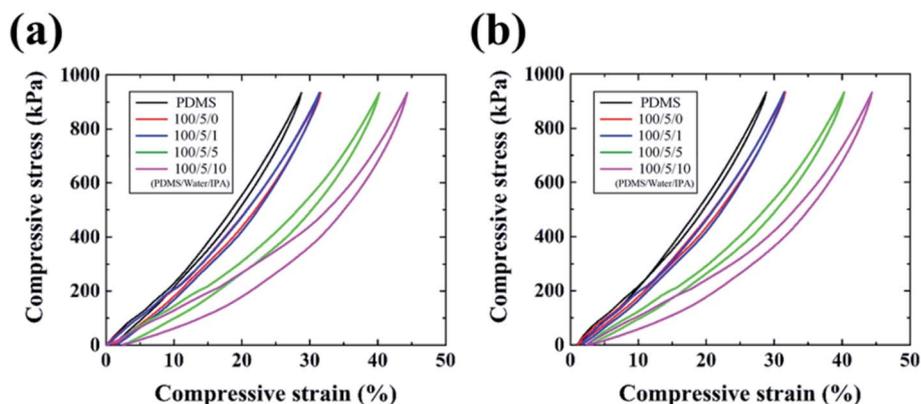

Fig. 4 Compressive stress–strain curves of PDMS and porous PDMS at (a) 1st cycle and (b) 3rd cycle. The enhanced flexibility of closed-cell porous PDMS in our study was derived by reducing the pore size.
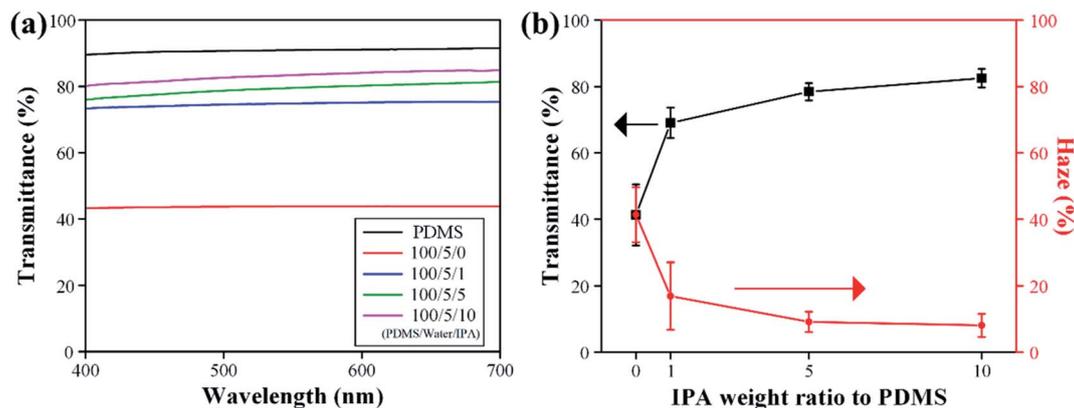
Fig. 5 (a) Optical transmittance spectra of PDMS and porous PDMS. (b) Transmittance (at 520 nm) and haze of porous PDMS. As the addition of IPA to water increases, the transparency and haze of porous PDMS significantly increases and decreases, respectively. This enhanced transparency was achieved by reducing the pore size to the submicron level.

flexibility. However, it is difficult to surely say which of the pore size and number density is more dominant in adjusting mechanical properties with the presented results. We are now further studying a method tuning the number density of pores with a similar size in PDMS, to confirm which one is more effective in adjusting mechanical properties. Meanwhile, similar viscoelastic behavior of the porous PDMS was obtained after repeated compression, as shown in Fig. 4a and b. The details of the repeated compressive stress–strain curves of porous PDMS (100/5/10) are presented in Fig. S6.† These results indicate that our approach is advantageous for achieving adjustable flexibility in PDMS.

Fig. 5 presents the optical properties of the fabricated porous PDMS. Porous PDMS prepared using only water exhibits low transparency of less than 50% in the visible light spectrum, which is comparable to the values of a study that reported using water as a porogen to form closed-cell porous PDMS.[26] However, with the addition of IPA to water, the transparency of porous PDMS increased significantly, as shown in Fig. 5a. This enhanced transparency could originate from the reduced pore size down to the submicron level considering that the light transmittance through porous materials increases in the spectrum below the wavelength of light.[54] The average transparency and haze of porous PDMS prepared with an added weight IPA ratio to PDMS of 0, 1 : 100, 5 : 100, and 10 : 100 were 41.32/41.40, 69.05/16.91, 78.44/9.16, and 82.56/8.06, respectively. We observed that optical haze defined as the ability to scatter transmitted light decreases as the added weight ratio of IPA increases. These results illuminate the highly advantageous aspect of our approach for adjusting the optical properties of porous PDMS. Meanwhile, the thickness of porous PDMS affect optical properties. The optical transmittance of porous PDMS with the different thicknesses (4 and 5 mm) is shown in Fig. S7.† Although the overall visible light transmittance decreases as the thickness of PDMS increases, we have confirmed the increasing tendency of transmittance as the added amount of IPA increases. This is originating from the reduction of pore size to lower light scattering, as mentioned in above. Additionally, the values of optical transparency and haze were obtained from a relatively bulky PDMS substrate having a thickness of 3

mm. Thus, the obtained values could be improved by reducing the thickness of the prepared PDMS to less than a millimeter based on the particular purpose. Fig. S8† shows the optical transmittance of porous PDMS prepared under the same conditions as the sample observed in Fig. 2. Moreover, the porous PDMS prepared by adding IPA shows the highest transparency compared to those obtained using other solvents. This also confirms the size of pores plays a crucial role in achieving increased transparency.

Thermal diffusivity of the fabricated porous PDMS, which is defined as the ratio of thermal conductivity to the product of density and specific heat capacity, is presented in Fig. 6 (refer to Fig. S9† which displays thermal diffusivity in a two-dimensional view). The measured thermal diffusivities of porous PDMS showed a decreasing tendency as the added weight ratio of IPA increased, except the 100/5/1 sample, regardless of the applied
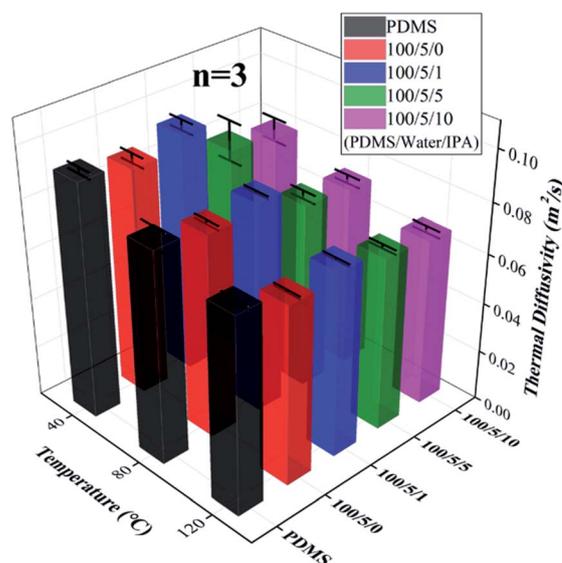

Fig. 6 Thermal diffusivity of porous PDMS. The measured thermal diffusivities of porous PDMS show a decreasing tendency as the added weight ratio of IPA increases, except 100/5/1 sample, regardless of the applied temperature ranging from 40 to 120 °C.

temperature ranging from 40 to 120 °C. As the porosity of porous media increases, the thermal conductivity decreases owing to phonon scattering at pore sites,[55] and the density of materials also decreases. Our porous PDMS prepared with different preparation methods exhibit similar porosity,[40] *i.e.*, show no significant difference in density, and hence the decrease in thermal diffusivity mainly would be induced by the decrease in thermal conductivity from phonon scattering. Thus, a higher number density of fine pores would indicate higher probabilities of phonon scattering, resulting in the decreased thermal conductivity. On the other hand, the size of pores also affects the thermal conductivity of porous material like the number density.[55] However, it is likewise difficult to say which of the pore size and number density is more dominant in adjusting thermal properties with the presented results. We are now further studying this like the aforementioned mechanical characterization. Even so, the lowered thermal conductivity and diffusivity of porous PDMS prepared with the added weight ratio of water (5 : 100) and IPA (10 : 100) may be favorable for a thermal insulator or a substrate of wearable heater requiring transparency and flexibility.[56,57] Additionally, we demonstrated that the thermal properties of porous PDMS are adjustable.

Hence, we expect that closed-cell porous PDMS can be candidate for a flexible and transparent material with improved mechanical flexibility, transparency, and thermal insulation. For example, a recently reported flexible thermoelectric generator uses structural support of porous PDMS as a flexible filler to maintain the difference in temperatures.[58] However, the used porous PDMS was not transparent. Thus, the presented porous PDMS with enhanced thermal insulation in this study can be used as the filler in the vertically-aligned thermoelectric generator,[59] requiring transparency and flexibility. Meanwhile, micro-voids in elastomers have received an attention as acoustic-wave absorbing materials in an underwater environment.[60,61] With the potential development of a method to fabricate periodic pores, our porous PDMS can be utilized for sound-absorbing materials. Another possible application of closed-cell PDMS could be impact energy absorbing materials with an addition of specific microspheres.[62] This addition would allow efficient energy absorption while taking advantage of the flexible and transparent properties of PDMS in this study.

Conclusions

In this study, we demonstrated fine-pored PDMS, whose pore size was reduced partially down to the submicron level. Various solvents were used and tested as co-solvents for dispersing water particles in the PDMS prepolymer to reduce the inner pore size. However, mixing IPA with water was most effective in reducing the pore size in the fabricated PDMS. Furthermore, solubility, surface tension, swelling ratio, and polarity of solvents were considered to analyze the mechanism of reducing the pore size when mixed with IPA and water in PDMS. Various weight ratios of IPA to uncured PDMS at constant water content were evaluated for developing porous PDMS with reduced size and increased number density of pores. The results indicated that the most reduced size and increased number density of pores were

obtained when the weight ratio of IPA (10 : 100) and water (5 : 100) were added to the prepolymer. Finally, adjustable mechanical, optical, and thermal properties of porous PDMS prepared with different ratios of IPA at a constant water ratio were presented. We observed that the flexibility/transparency and thermal diffusivity of the fabricated porous PDMS increased and decreased, as the size and number density of pores decreased and increased, respectively. This implies that the proposed method using IPA as an additional co-solvent in the water–pre-PDMS emulsion is highly advantageous for achieving improved flexibility, transparency, and thermal insulation properties. Given the simple fabrication process, cost-effectiveness, and enhanced flexibility/transparency, our approach of using porous PDMS as the substrate could be expected to be a promising candidate for various flexible and transparent electronics.

Conflicts of interest

There are no conflicts to declare.

Acknowledgements

Notes and references

1 T. Sannicolo, M. Lagrange, A. Cabos, C. Celle, J.-P. Simonato and D. Bellet, *Small*, 2016, **12**, 6052–6075.
2 H. B. Lee, W.-Y. Jin, M. M. Ovhal, N. Kumar and J.-W. Kang, *J. Mater. Chem. C*, 2019, **7**, 1087–1110.
3 Y. Fujisaki, H. Koga, Y. Nakajima, M. Nakata, H. Tsuji, T. Yamamoto, T. Kurita, M. Nogi and N. Shimidzu, *Adv. Funct. Mater.*, 2014, **24**, 1657–1663.
4 S. Das, R. Gulotty, A. V. Sumant and A. Roelofs, *Nano Lett.*, 2014, **14**, 2861–2866.
5 L. Zhou, H.-Y. Xiang, S. Shen, Y.-Q. Li, J.-D. Chen, H.-J. Xie, I. A. Goldthorpe, L.-S. Chen, S.-T. Lee and J.-X. Tang, *ACS Nano*, 2014, **8**, 12796–12805.
6 D.-Y. Kim, Y. C. Han, H. C. Kim, E. G. Jeong and K. C. Choi, *Adv. Funct. Mater.*, 2015, **25**, 7145–7153.
7 H. Choi, J. S. Choi, J.-S. Kim, J.-H. Choe, K. H. Chung, J.-W. Shin, J. T. Kim, D.-H. Youn, K.-C. Kim, J.-I. Lee, S.-Y. Choi, P. Kim, C.-G. Choi and Y.-J. Yu, *Small*, 2014, **10**, 3685–3691.
8 Z. Q. Zheng, J. D. Yao, B. Wang and G. W. Yang, *Sci. Rep.*, 2015, **5**, 11070.
9 J. Lee, M. Lim, J. Yoon, M. S. Kim, B. Choi, D. M. Kim, D. H. Kim, I. Park and S.-J. Choi, *ACS Appl. Mater. Interfaces*, 2017, **9**, 26279–26285.
10 S. Pyo, J. Choi and J. Kim, *Adv. Electron. Mater.*, 2018, **4**, 1700427.
11 B. W. An, S. Heo, S. Ji, F. Bien and J.-U. Park, *Nat. Commun.*, 2018, **9**, 2458.
12 S. Martin and B. Bhushan, *J. Colloid Interface Sci.*, 2017, **488**, 118–126.
13 J. Xu, W. Su, Z. Li, W. Liu, S. Liu and X. Ding, *J. Electroanal. Chem.*, 2017, **806**, 68–74.

14 N. Wang, Q. Wang, S. Xu and X. Zheng, *ACS Appl. Mater. Interfaces*, 2019, **11**, 48583–48593.

15 D. Zhu, S. Handschuh-Wang and X. Zhou, *J. Mater. Chem. A*, 2017, **5**, 16467–16497.

16 K. J. Cha and D. S. Kim, *Biomed. Microdevices*, 2011, **13**, 877.

17 X. Zhao, L. Li, B. Li, J. Zhang and A. Wang, *J. Mater. Chem. A*, 2014, **2**, 18281–18287.

18 S. Mohanty, K. Sanger, A. Heiskanen, J. Trifol, P. Szabo, M. Dufva, J. Emnéus and A. Wolff, *Mater. Sci. Eng. C*, 2016, **61**, 180–189.

19 S. Wu, J. Zhang, R. B. Ladani, A. R. Ravindran, A. P. Mouritz, A. J. Kinloch and C. H. Wang, *ACS Appl. Mater. Interfaces*, 2017, **9**, 14207–14215.

20 J. Li, X. Liu, J. M. Crook and G. G. Wallace, *Colloids Surf., B*, 2017, **159**, 386–393.

21 Q. Li, T. Duan, J. Shao and H. Yu, *J. Mater. Sci.*, 2018, **53**, 11873–11882.

22 J. González-Rivera, R. Iglio, G. Barillaro, C. Duce and M. R. Tinè, *Polymers*, 2018, **10**, 616.

23 W. Luo, M. Charara, M. C. Saha and Y. Liu, *Appl. Nanosci.*, 2019, **9**, 1309–1317.

24 M. Juchniewicz, D. Stadnik, K. Biesiada, A. Olszyna, M. Chudy, Z. Brzózka and A. Dybko, *Sens. Actuators, B*, 2007, **126**, 68–72.

25 S. Peng, P. G. Hartley, T. C. Hughes and Q. Guo, *Soft Matter*, 2012, **8**, 10493–10501.

26 B.-Y. Lee, J. Kim, H. Kim, C. Kim and S.-D. Lee, *Sens. Actuators, A*, 2016, **240**, 103–109.

27 A. Turco, E. Primiceri, M. Frigione, G. Maruccio and C. Malitesta, *J. Mater. Chem. A*, 2017, **5**, 23785–23793.

28 P. Thurgood, S. Baratchi, C. Szydzik, A. Mitchell and K. Khoshmanesh, *Lab Chip*, 2017, **17**, 2517–2527.

29 A. Davis, S. Surdo, G. Caputo, I. S. Bayer and A. Athanassiou, *ACS Appl. Mater. Interfaces*, 2018, **10**, 2907–2917.

30 R. Riesco, L. Boyer, S. Blosse, P. M. Lefebvre, P. Assemat, T. Leichle, A. Accardo and L. Malaquin, *ACS Appl. Mater. Interfaces*, 2019, **11**, 28631–28640.

31 L. Zhang, Y. Zhang, P. Chen, W. Du, X. Feng and B.-F. Liu, *Langmuir*, 2019, **35**, 11123–11131.

32 A. Vena, S. Kolle, S. Stafslien, J. Aizenberg and P. Kim, *Adv. Mater. Interfaces*, 2021, **8**, 2000359.

33 E. Favre, P. Schaetzel, Q. T. Nguygen, R. Clément and J. Néel, *J. Membr. Sci.*, 1994, **92**, 169–184.

34 J. Park, S. Wang, M. Li, C. Ahn, J. K. Hyun, D. S. Kim, D. K. Kim, J. A. Rogers, Y. Huang and S. Jeon, *Nat. Commun.*, 2012, **3**, 916.

35 C. Yu, C. Yu, L. Cui, Z. Song, X. Zhao, Y. Ma and L. Jiang, *Adv. Mater. Interfaces*, 2017, **4**, 1600862.

36 T. Zhou, J. Yang, D. Zhu, J. Zheng, S. Handschuh-Wang, X. Zhou, J. Zhang, Y. Liu, Z. Liu, C. He and X. Zhou, *Adv. Sci.*, 2017, **4**, 1700028.

37 S. Mohanty, L. B. Larsen, J. Trifol, P. Szabo, H. V. R. Burri, C. Canali, M. Dufva, J. Emnéus and A. Wolff, *Mater. Sci. Eng. C*, 2015, **55**, 569–578.

38 S. Kang, J. Lee, S. Lee, S. Kim, J.-K. Kim, H. Algadi, S. Al-Sayari, D.-E. Kim, D. Kim and T. Lee, *Adv. Electron. Mater.*, 2016, **2**, 1600356.

39 J. Chun, J. W. Kim, W.-s. Jung, C.-Y. Kang, S.-W. Kim, Z. L. Wang and J. M. Baik, *Energy Environ. Sci.*, 2015, **8**, 3006–3012.

40 Y. Kwak, E. Jo, Y. Kang and J. Kim, Highly Transparent Porous Polydimethylsiloxane with Micro-Size Pores Using Water and Isopropanol Mixture, presented in part at *the 2020 IEEE 33rd International Conference on Micro Electro Mechanical Systems (MEMS)*, Vancouver, Canada, 18–22 Jan. 2020.

41 M. D. Abràmoff, P. J. Magalhães and S. J. Ram, *Biophotonics International*, 2004, **11**, 36–42.

42 H. C. Chun, D. Giménez and S. W. Yoon, *Geoderma*, 2008, **146**, 83–93.

43 M. J. Large, S. P. Ogilvie, A. A. K. King and A. B. Dalton, *Langmuir*, 2017, **33**, 14766–14771.

44 J. N. Lee, C. Park and G. M. Whitesides, *Anal. Chem.*, 2003, **75**, 6544–6554.

45 T. Dong, E. P. Knoshaug, P. T. Pienkos and L. M. L. Laurens, *Appl. Energy*, 2016, **177**, 879–895.

46 Q. Bao, Y. Zou, Y. Wang, D. Kozak, S. Choi and D. J. Burgess, *J. Controlled Release*, 2019, **316**, 349–358.

47 J. Park, Y. Lee, M. H. Barbee, S. Cho, S. Cho, R. Shanker, J. Kim, J. Myoung, M. P. Kim, C. Baig, S. L. Craig and H. Ko, *Adv. Mater.*, 2019, **31**, 1808148.

48 A. Singh, B. D. Freeman and I. Pinnau, *J. Polym. Sci., Part B: Polym. Phys.*, 1998, **36**, 289–301.

49 S. J. Lue, C. L. Tsai, D.-T. Lee, K. P. O. Mahesh, M. Y. Hua, C.-C. Hu, Y. C. Jean, K.-R. Lee and J.-Y. Lai, *J. Membr. Sci.*, 2010, **349**, 321–332.

50 F. Goodarzi and S. Zendehboudi, *Can. J. Chem. Eng.*, 2019, **97**, 281–309.

51 A. Rinaldi, A. Tamburrano, M. Fortunato and M. S. Sarto, *Sensors*, 2016, **16**, 2148.

52 A. Kovalenko, K. Zimny, B. Mascaro, T. Brunet and O. Mondain-Monval, *Soft Matter*, 2016, **12**, 5154–5163.

53 S. Zhao and R. Zhu, *Adv. Mater. Technol.*, 2017, **2**, 1700183.

54 S. Pérez-Tamarit, B. Notario, E. Solórzano and M. A. Rodriguez-Perez, *Mater. Lett.*, 2018, **210**, 39–41.

55 S. S. Sundarram and W. Li, *Polym. Eng. Sci.*, 2013, **53**, 1901–1909.

56 R. D. I. G. Dharmasena, K. D. G. I. Jayawardena, Z. Saadi, X. Yao, R. M. I. Bandara, Y. Zhao and S. R. P. Silva, *Proc. IEEE*, 2019, **107**, 2118–2136.

57 S. Hong, H. Lee, J. Lee, J. Kwon, S. Han, Y. D. Suh, H. Cho, J. Shin, J. Yeo and S. H. Ko, *Adv. Mater.*, 2015, **27**, 4744–4751.

58 S.-J. Jung, J. Shin, S.-S. Lim, B. Kwon, S.-H. Baek, S. K. Kim, H.-H. Park and J.-S. Kim, *Nano Energy*, 2021, **81**, 105604.

59 B. M. M. Faustino, D. Gomes, J. Faria, T. Juntunen, G. Gaspar, C. Bianchi, A. Almeida, A. Marques, I. Tittonen and I. Ferreira, *Sci. Rep.*, 2018, **8**, 6867.

60 V. Leroy, A. Strybulevych, M. Lanoy, F. Lemoult, A. Tourin and J. H. Page, *Phys. Rev. B*, 2015, **91**, 020301.

61 Y. Fu, J. Fischer, K. Pan, G. H. Yeoh and Z. Peng, *Appl. Acoust.*, 2021, **171**, 107668.

62 J.-H. Cai, M.-L. Huang, X.-D. Chen and M. Wang, *Appl. Surf. Sci.*, 2021, **540**, 148364.